Quadrupedal Locomotion via Event-Based Predictive Control and QP-Based Virtual Constraints

Kaveh Akbari Hamed, Jeeseop Kim, and Abhishek Pandala

***Abstract*—This letter aims to develop a hierarchical nonlinear control algorithm, based on model predictive control (MPC), quadratic programming (QP), and virtual constraints, to generate and stabilize locomotion patterns in a real-time manner for dynamical models of quadrupedal robots. The higher level of the proposed control scheme is developed based on an event-based MPC that computes the optimal center of mass (COM) trajectories for a reduced-order linear inverted pendulum (LIP) model subject to the feasibility of the net ground reaction force (GRF). The asymptotic stability of a desired target point for the reduced-order model under the event-based MPC approach is investigated. It is shown that the event-based nature of the proposed MPC approach can significantly reduce the computational burden associated with the real-time implementation of MPC techniques. To bridge the gap between reduced- and full-order models, QP-based virtual constraint controllers are developed at the lower level of the proposed control scheme to impose the full-order dynamics to track the optimal trajectories while having all individual GRFs in the friction cone. The analytical results of the letter are numerically verified to demonstrate stable and robust locomotion of a 22 degree of freedom quadrupedal robot, in the presence of payloads, external disturbances, ground height variations, and uncertainty in contact models.**

***Index Terms*—Legged robots, motion control, multi-contact whole-body motion planning and control.**

I. Introduction

THE overarching goal of this paper is to develop a hierarchical control algorithm, based on nonlinear control, model predictive control (MPC), and quadratic programming (QP), to generate and stabilize locomotion trajectories for complex dynamical models of quadrupedal robots in a real-time manner. The proposed approach employs a higher-level and event-based MPC at the beginning of each continuous-time domain (i.e., event) that generates optimal trajectories for a reduced-order linear inverted pendulum (LIP) model subject to the feasibility of the net ground reaction force (GRF). The stability of the system subject to event-based MPC is investigated to demonstrate that the MPC does not need to be solved at every time sample. This significantly reduces the computational burden associated with MPC-based path planning approaches of legged locomotion while guaranteeing stability. To reduce the difference between the reduced- and full-order models of locomotion, a QP-based nonlinear controller is solved at the lower level of the proposed approach to impose the full-order dynamics to track the optimal trajectories while keeping all individual GRFs feasible. It is shown that the developed control algorithm can result in stable and robust locomotion patterns in the presence of payloads, external disturbances, and model uncertainties.

Manuscript received February 19, 2020; accepted May 30, 2020. Date of publication June 10, 2020; date of current version June 18, 2020. This letter was recommended for publication by Associate Editor M. Hutter and Editor A. Kheddar upon evaluation of the reviewers' comments. The work of K. Akbari Hamed was supported by the National Science Foundation under Grants 1906727, 1923216, and 1924617. The work of J. Kim and A. Pandala was supported by the National Science Foundation under Grant 1854898. *(Corresponding author: Kaveh Akbari Hamed.)*

The authors are with the Department of Mechanical Engineering, Virginia Tech, Blacksburg, VA 24061 USA (e-mail: kavehakbarihamed@vt.edu; jeeseop@vt.edu; agp19@vt.edu).

This letter has supplementary downloadable material available at https://ieeexplore.ieee.org, provided by the authors.

Digital Object Identifier 10.1109/LRA.2020.3001471

A. Related Work and Motivation

Hybrid systems theory has become a powerful approach for modeling and control of legged locomotion [1]–[12]. Existing nonlinear control techniques that address the hybrid nature of locomotion models have been developed based on hybrid reduction [13], controlled symmetries [8], transverse linearization [9], and hybrid zero dynamics (HZD) [2], [14]. In the HZD approach, a set of kinematic constraints, referred to as virtual constraints, is defined to coordinate the links of the robot within a stride. The virtual constraints are imposed by the action of a feedback controller (e.g., input-output (I-O) linearization [15]). The virtual constraint controllers have been numerically and experimentally validated for the motion control of bipedal robots [2], [3], [6], [16]–[19], powered prosthetic legs [20], [21] and exoskeletons [22]. The gait planning in the HZD approach is typically formulated as a nonlinear programming (NLP) problem. Reference [18] developed a scalable gait planning approach based on HZD and direct collocation (see e.g., [23] for quadrupedal locomotion). Although the direct-collocation based HZD approach generates trajectories for full-order models of locomotion in a fast manner, it *cannot* address real-time trajectory optimization in complex environments.

MPC-based approaches integrated with reduced-order models have been used for real-time path planning of bipedal and quadrupedal locomotion, see e.g., [24]–[27]. Most of these approaches address linear inverted pendulum (LIP) models for bipedal locomotion while generating optimal trajectories for the center of mass (COM) and center of pressure (COP) of the robot subject to the zero moment point (ZMP) conditions [28] and feasibility of the GRF. These techniques, however, cannot be easily extended to quadrupedal locomotion as the LIP-based MPC approaches do *not* consider the feasibility of all individual GRFs. To tackle this problem, [29]–[31] have developed an interesting

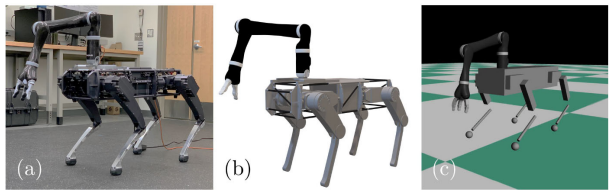

Fig. 1. Vision 60 augmented with Kinova arm (a) together with its CAD representation (b) and full-order model in RaiSim (c).

convex optimization formulation based on MPC and centroidal dynamics. In particular, the MPC approach of [29]–[31] plans for the optimal GRFs of the contacting leg ends at every time sample (e.g., 200 Hz) for agile quadrupedal locomotion. Alternative interesting approaches for agile locomotion have utilized nonlinear MPC [32], policy-regularized MPC [33], and QP-based whole-body control [34], [35]. Although state-of-the-art techniques for MPC-based control of quadrupedal locomotion have shown a very good level of robustness, they require solving MPC at every time sample. These MPC problems are typically formulated as convex QPs for robot with light legs and may have a significant number of decision variables to be optimized. This makes the MPC-based techniques computationally intensive. The paper aims to develop control algorithms with less computational load for which the MPC problems do not need to be solved every time sample. We would like to answer the following *questions:* 1) how can we implement an MPC-based approach for planning of legged locomotion at a slower rate while guaranteeing the stability and robustness of the gaits, and 2) how can we systematically bridge the gap between the reduced- and full-order models using the HZD approach for robots with heavy legs like Vision 60 (see Fig. 1)? The paper also aims to show that these controllers are robust enough to stabilize locomotion despite a slow replan rate. A potential application for this event-based MPC scheme can be in the context of networked or distributed control systems for collaborative quadrupedal robots, where reducing the amount of computation is of great interest [36].

B. Objectives and Contributions

The *objectives* and *key contributions* of this paper are as follows. The paper develops a hierarchical control algorithm based on an event-based MPC and QP-based virtual constraint controllers that generate and stabilize quadrupedal locomotion patterns in real time (see Fig. 2a). In particular, we do not employ any NLP-based and computationally expensive HZD gait planning algorithm. The higher level of the proposed approach formulates a finite-time and QP-based MPC at the beginning of each continuous-time domain (i.e., event-based manner) to compute the optimal COM trajectories subject to the net GRF feasibility. This can address any locomotion pattern in different directions (e.g., forward, backward, sideways, in-place, and diagonal) via any predefined contact sequences with possible start and stop conditions. The stability of the target point for the LIP model with the proposed event-based MPC is addressed. It is shown that under some sufficient conditions, one would not need to solve the MPC problem at every-time sample to reach the target point. This significantly reduces the computational complexity of real-time MPC. To bridge the gap between the LIP and full-order model of locomotion, a low-level and QP-based virtual constraints controller is developed. The low-level controller imposes the full-order dynamics to track the optimal reduced-order trajectories while having all individual GRFs in the friction cone. Additionally, the lower-level QP has fewer decision variables compared to the event-based MPC (e.g., 50%). The analytical results of the paper are numerically confirmed on full-order simulation models of a 22 DOF quadrupedal robot, Vision 60, that is augmented by a Kinova manipulator (see Fig. 1). The paper also investigates the robustness of the proposed control algorithm against 1) payloads, 2) external disturbances, 3) ground height variations, and 4) different contact modeling approaches. It is shown that the proposed controller can systematically generate and stabilize gaits in different directions. In [37], the authors presented an interesting LIP-based and nonlinear trajectory optimization framework to generate a wide range of quadrupedal gaits. The approach of the current paper completely differs from [37] in that 1) we address event-based MPC for trajectory planning of the LIP model while addressing the asymptotic stability of the final target point, and 2) we reduce the gap between the reduced- and full-order dynamical models by setting up the QP-based virtual constraint controllers. Unlike the two-level control approach of [38], the current paper 1) studies the asymptotic stability under the MPC approach, and then 2) extends the concept of HZD controllers, based on convex optimization, to quadrupedal locomotion.

II. Models of Legged Locomotion

We consider a full-order dynamical model of Vision 60 that is augmented by a Kinova robotic manipulator for locomotion and manipulation purpose. Vision 60 is a quadrupedal robot manufactured by Ghost Robotics. The floating-base model of the composite robot consists of 22 degrees of freedom (DOFs) of which 12 DOFs are actuated and assigned to legs. In particular, each leg of the robot has an actuated 2 DOF hip joint plus an actuated 1 DOF knee joint and ends at a point foot. In addition, 4 DOFs with 4 actuators are assigned to the Kinova manipulator. The remaining 6 DOFs are unactuated and describe the absolute position and orientation of the robot with respect to an inertial world frame. The generalized coordinates of the robot can be expressed as $q := \text{col}(p_b, \phi_b, q_{\text{body}}) \in \mathcal{Q} \subset \mathbb{R}^{22}$, in which $p_b \in \mathbb{R}^3$ and $\phi_b \in \mathbb{R}^3$ describe the absolute position and orientation of the torso, respectively. Moreover, $q_{\text{body}} \in \mathbb{R}^{16}$ represents the shape (i.e., internal joints) of the robot. The state vector of the mechanical system is taken as $x := \text{col}(q, \dot{q}) \in \mathcal{X}$, where $\mathcal{X} := \text{T}\mathcal{Q} := \mathcal{Q} \times \mathbb{R}^{22}$ denotes the state space. In our notation, "col" represents the column vector. The control inputs (i.e., joint torques) are finally represented by $\tau \in \mathbb{R}^{16}$. The evolution of the robot can be expressed by the following ordinary differential equations (ODEs)

$$D(q)\,\ddot{q} + H\,(q, \dot{q}) = \Upsilon\,\tau + \sum_{\ell \in \mathcal{C}} J_\ell^\top\,(q)\,F_\ell, \tag{1}$$

where $D(q) \in \mathbb{R}^{22\times 22}$ represents the positive definite mass-inertia matrix, $H(q, \dot{q}) \in \mathbb{R}^{22}$ denotes the Coriolis, centrifugal,

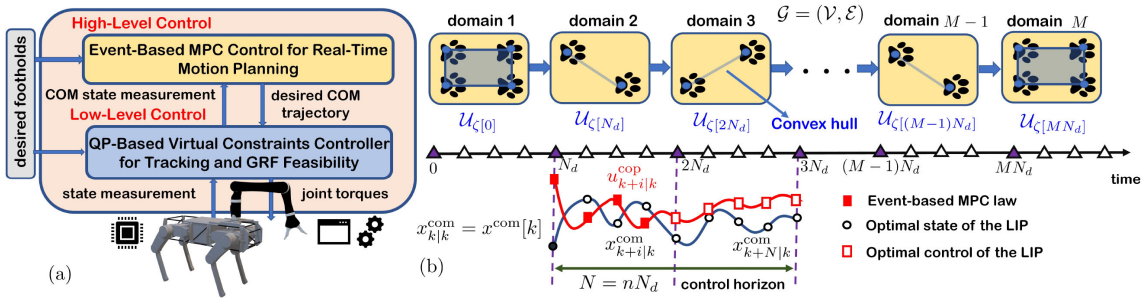

Fig. 2. (a) Illustration of the proposed hierarchical control algorithm, based on nonlinear control, QP, and event-based MPC. (b) Illustration of a locomotion pattern with the corresponding graph $\mathcal{G}=(\mathcal{V},\mathcal{E})$ and the event-based MPC law.

and gravitational forces, and $\Upsilon \in \mathbb{R}^{22\times 16}$ represents the input distribution matrix. In our notation, $\mathcal{C}$ is the index set of contact points with the ground. Furthermore, for every $\ell \in \mathcal{C}$, $J_\ell(q) \in \mathbb{R}^{3\times 22}$ and $F_\ell \in \mathbb{R}^3$ denote the corresponding contact Jacobian matrix and GRF, respectively. The contact forces can be computed using 1) the rigid contact assumption and hybrid system approach [23], [39], 2) compliant contact models (e.g., LuGre model [40]), or 3) nonlinear and linear complementarity problems [41] as well as optimization-based techniques [42], [43]. We remark that the model (1) is valid if $F_\ell \in \mathcal{FC}$ for all $\ell \in \mathcal{C}$, where $\mathcal{FC} := \{(F_x, F_y, F_z)^\top \,|\, F_z > 0,\ \pm F_x < \frac{\mu}{\sqrt{2}} F_z,\ \pm F_y < \frac{\mu}{\sqrt{2}} F_z\}$ denotes the friction cone for some friction coefficient μ. For later purposes, the equations of motion in (1) can be written in a state space form as

$$\dot{x} = f(x) + g(x)\,\tau + w(x)\,F, \tag{2}$$

in which $F := \text{col}\{F_\ell \,|\, \ell \in \mathcal{C}\}$ represents the contact forces.

III. Event-Based Predictive Control

In this letter, we develop a two-level control algorithm that can steer a quadrupedal robot from an initial point to a final point in a stable and robust manner (see Fig. 2a). At the higher level of the control algorithm, we employ an event-based MPC for real-time motion planning of the COM. In particular, we formulate a finite-time optimal control problem based on MPC and convex QP to steer the state of a reduced-order LIP model subject to the feasibility of the net GRF. The lower-level controller is developed based on the concept of virtual constraints and QP and will be presented in Section V.

Reduced-Order LIP Model: The LIP model can be described by the following ODEs [26]

$$\begin{bmatrix} \ddot{r}_x^{\text{com}} \\ \ddot{r}_y^{\text{com}} \end{bmatrix} = \frac{g_0}{r_z^{\text{com}}} \begin{bmatrix} r_x^{\text{com}} - u_x^{\text{cop}} \\ r_y^{\text{com}} - u_y^{\text{cop}} \end{bmatrix}, \tag{3}$$

where $r^{\text{com}} := \text{col}(r_x^{\text{com}}, r_y^{\text{com}}) \in \mathbb{R}^2$ denotes the Cartesian coordinates of the COM with respect to the inertial world frame, projected onto the xy-plane, r_z^{com} represents the constant height of the COM, g_0 is the gravitational constant, and $u^{\text{cop}} := \text{col}(u_x^{\text{cop}}, u_y^{\text{cop}}) \in \mathbb{R}^2$ denotes the Cartesian coordinates of the COP. From (3), the net GRF applied to the COM can be expressed as $F_{\text{net}} := \sum_{\ell\in\mathcal{C}} F_\ell = m_{\text{tot}}\,\text{col}(\ddot{r}_x^{\text{com}}, \ddot{r}_y^{\text{com}}, g_0)$, in which m_{tot} represents the total mass of the robot. By defining the LIP state vector $x^{\text{com}} := \text{col}(r_x^{\text{com}}, \dot{r}_x^{\text{com}}, r_y^{\text{com}}, \dot{r}_y^{\text{com}}) \in \mathbb{R}^4$ and employing the zero-order hold (ZOH) discretization approach for some sampling time T_d, the ODEs in (3) can be discretized as follows

$$x^{\text{com}}[k+1] = A_d\, x^{\text{com}}[k] + B_d\, u^{\text{cop}}[k], \tag{4}$$

where $k \in \mathbb{Z}_{\geq 0}$ represents a non-negative integer with $A_d \in \mathbb{R}^{4\times 4}$ and $B_d \in \mathbb{R}^{4\times 2}$ being the state and input matrices, respectively.

Steering Problem: We are interested in steering the discrete-time dynamics (4) from an initial state to a final state over M continuous-time domains for some positive integer $M \geq 1$. We consider a general locomotion pattern with an arbitrary sequence of double-, triple-, or quadruple-contact domains. Unlike our previous work [23], the locomotion pattern does *not* need to be cyclic. In particular, we address general locomotion with start and stop options. To make this notion more precise, we consider a directed graph $\mathcal{G} = (\mathcal{V}, \mathcal{E})$ for the desired locomotion pattern, whose *vertex set* represents the ordered sequence of continuous-time domains. In addition, $\mathcal{E} \subset \mathcal{V} \times \mathcal{V}$ denotes the *edge set* to represent transitions (see Fig. 2b). Let us suppose that each continuous-time domain consists of $N_d \geq 1$ time samples (i.e., grid points). We then define the *domain indicator function* as $\zeta : \mathbb{Z}_{\geq 0} \to \{1, 2, \ldots, M\}$ by $\zeta[k] := \lfloor \frac{k}{N_d} \rfloor + 1$ for $0 \leq k < MN_d$ and $\zeta[k] := M$ for $k \geq MN_d$ to assign the domain index for every time sample $k \in \mathbb{Z}_{\geq 0}$. Here, $\lfloor . \rfloor$ represents the floor function. For the feasibility of the model, we assume that the input $u^{\text{cop}}[k]$ lies in the support polygon which is defined as the convex hull of the contacting points with the ground. That is, $u^{\text{cop}}[k] \in \mathcal{U}_{\zeta[k]}$ for all $k \in \mathbb{Z}_{\geq 0}$, where $\mathcal{U}_{\zeta[k]} \subset \mathbb{R}^2$ is the corresponding convex hull for the domain $\zeta[k]$ (see Fig. 2b). If we define the *contact coordinates matrix* for the domain $\zeta[k]$ as $C_{\zeta[k]}$ whose columns represent the Cartesian coordinates of the contacting feet with the ground, $u^{\text{cop}}[k] \in \mathcal{U}_{\zeta[k]}$ is equivalent to the existence of a time-varying vector $\lambda[k]$ such that

$$\mathbf{0} \leq \lambda[k] \leq \mathbf{1},\ \ \mathbf{1}^\top \lambda[k] = 1,\ \ u^{\text{cop}}[k] = C_{\zeta[k]}\lambda[k]. \tag{5}$$

We remark that in our notation, $\mathbf{0}$ and $\mathbf{1}$ denote vectors whose elements are zero and one, respectively. In addition, for the feasibility of the LIP model, the net force must lie in the friction cone, i.e., $F_{\text{net}} \in \mathcal{FC}$. This latter condition together with (3) can be expressed as

$$\Phi\, x^{\text{com}}[k] + \Psi\, u^{\text{cop}}[k] \leq \eta, \quad \forall k \in \mathbb{Z}_{\geq 0} \tag{6}$$

for some proper Φ and Ψ matrices and some proper η vector.

Problem 1 (Optimal Steering Problem): For a given locomotion graph $\mathcal{G}$, a phase index function ζ, a set of known contact coordinates matrices $\{C_{\zeta[k]}\}_{k\in\mathbb{Z}_{\geq 0}}$, an initial state x_0^{com}, a final state x_f^{com}, and a steering time $T_f \in \mathbb{Z}_{\geq 0}$, the optimal steering problem consists of finding an optimal sequence of control (i.e., COP) inputs $u^{\text{cop}}[k]$ for $0 \leq k \leq T_f - 1$ that steer (4) from x_0^{com} to x_f^{com} subject to (5) and (6).

Event-Based MPC: To address Problem 1, we set up an event-based MPC that is solved at the beginning of each domain (i.e., event) with some control horizon $N = nN_d$ and $n \geq 1$. In particular, for every time sample $k = mN_d$ with $m \in \mathbb{Z}_{\geq 0}$, we consider the following finite-time optimal control problem

$$\begin{aligned}
&\min_{U^{\text{cop}}_{k\to k+N-1|k}} \ \mathcal{J}_k\left(x^{\text{com}}[k], U^{\text{cop}}_{k\to k+N-1|k}\right)\\
&= p\left(x^{\text{com}}_{k+N|k}\right) + \sum_{i=0}^{N-1}\mathcal{L}\left(x^{\text{com}}_{k+i|k}, u^{\text{cop}}_{k+i|k}\right)\\
&\text{s.t.} \qquad x^{\text{com}}_{k+i+1|k} = A_d\, x^{\text{com}}_{k+i|k} + B_d\, u^{\text{cop}}_{k+i|k}\\
&\qquad\quad \Phi\, x^{\text{com}}_{k+i|k} + \Psi\, u^{\text{cop}}_{k+i|k} \leq \eta\\
&\qquad\quad u^{\text{cop}}_{k+i|i} \in \mathcal{U}_{\zeta[k+i]} i = 0, 1, \ldots, N-1, \qquad (7)
\end{aligned}$$

where $U^{\text{cop}}_{k\to k+N-1|k} := \text{col}(u^{\text{cop}}_{k|k}, \ldots, u^{\text{cop}}_{k+N-1|k})$ and $x^{\text{com}}_{k+i|k}$ represents the estimated state vector at time $k+i$ predicted at time k according to the recursive law $x^{\text{com}}_{k+i+1|k} = A_d\, x^{\text{com}}_{k+i|k} + B_d\, u^{\text{cop}}_{k+i|k}$ starting from the current state $x^{\text{com}}_{k|k} := x^{\text{com}}[k]$. In an analogous manner, $u^{\text{cop}}_{k+i|k}$ denotes the COP input at time $k+i$ computed at time k. Furthermore, $p(x^{\text{com}}_{k+N|k})$ and $\mathcal{L}(x^{\text{com}}_{k+i|k}, u^{\text{cop}}_{k+i|k})$ are the terminal and stage costs, respectively, defined as $p(x^{\text{com}}_{k+N|k}) := \|x^{\text{com}}_{k+N|k} - d^{\text{com}}_{k+N|k}\|^2_P$ and $\mathcal{L}(x^{\text{com}}_{k+i|k}, u^{\text{cop}}_{k+i|k}) := \|x^{\text{com}}_{k+i|k} - d^{\text{com}}_{k+i|k}\|^2_Q + \|u^{\text{cop}}_{k+i|k}\|^2_R$ for some positive definite matrices $P \in \mathbb{R}^{4\times 4}$, $Q \in \mathbb{R}^{4\times 4}$, and $R \in \mathbb{R}^{2\times 2}$, in which $\|z\|^2_P := z^\top P z$. In our notation, $d^{\text{com}}_{k+i|k}$ represents a desired state trajectory for $x^{\text{com}}_{k+i|k}$ that is smooth in i (e.g., linear) while starting at the current state $x^{\text{com}}[k]$ and ending at the final state x_f^{com}. Let $U^\star_{k\to k+N-1|k} := \text{col}(u^{\star\text{cop}}_{k|k}, \ldots, u^{\star\text{cop}}_{k+N-1|k})$ be the optimal solution of the problem (7). Then in our proposed approach, the first N_d components of $U^\star_{k\to k+N-1|k}$, that correspond to the time samples of the current continuous-time domain, are employed to the system (4) (see Fig. 2b), that is,

$$u^{\text{cop}}[k+j] = u^{\star\text{cop}}_{k+j|k}, \quad j = 0, 1, \ldots, N_d - 1. \qquad (8)$$

For later purposes, we assume that $\pi_j(k, x^{\text{com}}[k]) := u^{\star\text{cop}}_{k+j|k}$ for $j = 0, 1, \ldots, N_d - 1$ represents the MPC law computed at time k (see again Fig. 2b). The evolution of the closed-loop LIP model can then be expressed as

$$\begin{aligned}
x^{\text{com}}[mN_d + j] &= A_d^j\, x^{\text{com}}[mN_d]\\
&\quad + \sum_{\ell=0}^{j-1} A_d^{j-1-\ell} B_d\, \pi_\ell\left(mN_d, x^{\text{com}}[mN_d]\right), \qquad (9)
\end{aligned}$$

for every $m \in \mathbb{Z}_{\geq 0}$ and $j = 0, 1, \ldots, N_d$. In addition, we can define the following *down-sample closed-loop system*

$$\begin{aligned}
x^{\text{com}}[(m+1)N_d] &= A_d^{N_d}\, x^{\text{com}}[mN_d]\\
&\quad + \sum_{\ell=0}^{N_d-1} A_d^{N_d-1-\ell} B_d\, \pi_\ell\left(mN_d, x^{\text{com}}[mN_d]\right)\\
&=: \Delta_{\text{down}}\left(mN_d, x^{\text{com}}[mN_d]\right) \qquad (10)
\end{aligned}$$

for all $m \in \mathbb{Z}_{\geq 0}$ whose state is updated every N_d samples.

Remark 1: We remark that the MPC formulation (7) together with (5) can be expressed as QP in terms of the decisions variables $\{x^{\text{com}}_{k+i|k}\}_{i=1}^{N}$, $\{u^{\text{cop}}_{k+i|k}\}_{i=0}^{N-1}$, and $\{\lambda_{k+i|k}\}_{i=0}^{N-1}$ to retain the sparsity structure of [44]. To make the cost function of this QP positive definite in terms of all decision variables, one can add a term corresponding to $\lambda_{k+i|k}$, i.e., $\mathcal{J}_k = p(x^{\text{com}}_{k+N|k}) + \sum_{i=0}^{N-1}\mathcal{L}(x^{\text{com}}_{k+i|k}, u^{\text{cop}}_{k+i|k}) + \mathcal{H}(\lambda_{k+i|k})$, where $\mathcal{H}(\lambda_{k+i|k}) := \|\lambda_{k+i|k} - \lambda^{\text{des}}_{k+i|k}\|^2_{\hat{R}}$ for some desired trajectory $\lambda^{\text{des}}_{k+i|k}$ and some positive definite matrix $\hat{R}$.

IV. Asymptotic Stability Analysis

The objective of this section is to address the asymptotic stability property of the target state for the closed-loop system. We aim to establish a connection between the asymptotic stability of the target state for the down-sample closed-loop system and that of the the original closed-loop system. Without loss of generality, we assume that the target state is taken at the origin, i.e., $x_f^{\text{com}} = 0$. We then make the following assumption.

Assumption 1: The MPC problem is formulated as QP with a positive definite cost function as mentioned in Remark 1. In addition, the MPC is feasible for every $k = mN_d$ with optimal laws satisfying the conditions $\pi_j(mN_d, 0) = 0$ for all $m \in \mathbb{Z}_{\geq 0}$ and $j = 0, 1, \ldots, N_d - 1$.

Lemma 1. (Lipschitz Continuity): Suppose that Assumption 1 is satisfied. Then, the MPC laws are locally Lipschitz in x^{com}, i.e., there exists $\rho_{m,j} > 0$ for all $m \in \mathbb{Z}_{\geq 0}$ and $j = 0, 1, \ldots, N_d - 1$ such that $\|\pi_j(mN_d, x^{\text{com}})\| \leq \rho_{m,j}\|x^{\text{com}}\|$ for all x^{com} in an open neighborhood of the origin.

Proof: We can show that the QP problem of Remark 1 can be expressed as a canonical QP (CQP) [45], that is, $\min_\xi\{\frac{1}{2}\xi^\top\mathcal{P}\xi + \psi(x^{\text{com}})^\top\xi |\, \mathcal{A}\,\xi \geq \phi(x^{\text{com}}), \xi \geq 0\}$ with some positive definite matrix $\mathcal{P}$, a matrix $\mathcal{A}$, and some vectors $\psi(x^{\text{com}})$ and $\phi(x^{\text{com}})$ that depend smoothly on the current state x^{com} of the LIP model. Applying [45, Theorem 2.1] together with $\pi_j(mN_d, 0) = 0$ completes the proof. ■

Now we are in a position to present the following theorem.

Theorem 1. (Stability Analysis based on the Down-Sample System): Consider the original and down-sample discrete-time systems (9) and (10) with the MPC laws satisfying Assumption 1. Suppose further that the Lipschitz constants $\rho_{m,j}$ are bounded for all $m \in \mathbb{Z}_{\geq 0}$ and all $j = 0, 1, \ldots, N_d - 1$, that is, $\rho_{m,j} \leq \rho$ for some $\rho > 0$. If the origin is uniformly asymptotically stable for the down-sample discrete-time system (10), then it is asymptotically stable for the original system (9).

Proof: Since the origin is uniformly asymptotically stable for the down-sample system (10), there is a class $\mathcal{KL}$ function β

such that $\|x^{\text{com}}[mN_d]\| \leq \beta(\|x^{\text{com}}[0]\|, mN_d)$ for all $m \in \mathbb{Z}_{\geq 0}$ and every initial condition in an open neighborhood of the origin. From (9) and Lemma 1, one can conclude that

$$\begin{aligned}\|x^{\text{com}}[mN_d + j]\| &\leq \|A_d^j\|\, \|x^{\text{com}}[mN_d]\| \\ &\quad + \sum_{\ell=0}^{j-1} \|A_d^{j-1-\ell}\| \|B_d\|\, \rho\, \|x^{\text{com}}[mN_d]\| \\ &\leq L_j\, \beta\left(\|x^{\text{com}}[0]\|, mN_d\right), \end{aligned} \tag{11}$$

where $L_j := \|A_d^j\| + \rho \sum_{\ell=0}^{j-1} \|A_d^{j-1-\ell}\| \|B_d\|$ for $j = 0, 1, \ldots, N_d - 1$. By defining, $L := \max\{L_j \,|\, 0 \leq j \leq N_d - 1\}$, inequality (11) becomes $\|x^{\text{com}}[mN_d + j]\| \leq L\, \beta(\|x^{\text{com}}[0]\|, mN_d)$. For a given $\epsilon > 0$, one can choose $\delta > 0$ such that $L\, \beta(\delta, 0) < \epsilon$. Then, from properties of class $\mathcal{KL}$ functions, $\|x^{\text{com}}[mN_d + j]\| \leq L\, \beta(\|x^{\text{com}}[0]\|, 0) < \epsilon$ for every $\|x^{\text{com}}[0]\| < \delta$ and all $m \in \mathbb{Z}_{\geq 0}$ and $j = 0, 1, \ldots, N_d - 1$ which concludes the stability. Furthermore, $\lim_{m\to\infty} \|x^{\text{com}}[mN_d + j]\| = 0$ for all $\|x^{\text{com}}[0]\| < \delta$ which completes the proof of asymptotic stability. ■

V. QP-Based HZD Controllers

The objective of this section is to develop the low-level control algorithm based on QP and the virtual constraints approach. In particular, we would like to develop a nonlinear control algorithm to track the optimal COM trajectory that is generated by the higher-level MPC for the current continuous-time domain. The low-level controller also imposes the swing legs to follow an appropriate path to land at the desired footholds. The trajectory tracking problem is formulated via the virtual constraints approach. Since the higher-level LIP model only considers the feasibility of the net force F_{net}, the lower-level controller formulates the I-O linearization problem as a QP that addresses the feasibility of all individual contact forces F_ℓ for $\ell \in \mathcal{C}$ while tracking the LIP trajectories.

Virtual Constraints: In this letter, we define a set of time-varying and holonomic virtual constraints as follows

$$y(x,t) := h(q,t) := h_0(q) - h_d\left(s, \alpha\right), \tag{12}$$

in which $h_0(q)$ denotes a set of holonomic quantities to be controlled. In addition, $h_d(s,\alpha)$ represents the desired evolution of the controlled variables in terms of the phasing variable s. Here, $s := \frac{t - t^+}{N_d\, T_d}$ denotes the phasing variable with t^+ being the initial time for the current domain and $N_d T_d$ representing an estimated elapsed time for the domain. The desired trajectory $h_d(s,\alpha)$ is taken as a Bézier polynomial with a coefficient matrix α. During the quadruple-contact domains, we choose $h_0(q) \in \mathbb{R}^6$ as the roll, pitch, and yaw angles of the torso together with the COM positions. The idea is to regulate the absolute orientation of the robot while imposing the COM coordinates to follow the optimal COM trajectory generated by the MPC. Here, the coefficient matrix α can be chosen via least squares at the beginning of each domain such that $h_d(s,\alpha)$ has the best fit to the optimal COM trajectory over N_d samples. For double- and triple-contact domains, $h_0(q)$ is augmented with the Cartesian coordinates of the swing leg ends for foot placement. The idea is to follow a desired foot trajectory in the workspace starting from the previous foothold and ending at the next preplanned foothold. This makes the output function 12- and 9-dimensional for the double- and triple-contact domains, respectively. To control the configuration of the manipulator, we augment $h_0(q)$ and $h_d(s,\alpha)$ by the Cartesian coordinates of the end-effector (EE) and its desired trajectory in the workspace, respectively.

QP-Based I-O Linearization: Differentiating the output functions (12) along (2) results in the following output dynamics

$$\begin{aligned}\ddot{y} &= \mathrm{L}_g\mathrm{L}_f y(x,t)\, \tau + \mathrm{L}_w\mathrm{L}_f y(x,t)\, F \\ &\quad + \mathrm{L}_f^2 y(x,t) + \frac{\partial^2 y}{\partial t^2}(x,t) \\ &= -K_D\, \dot{y} - K_P\, y, \end{aligned} \tag{13}$$

in which $\mathrm{L}_g\mathrm{L}_f y, \mathrm{L}_w\mathrm{L}_f y$, and $\mathrm{L}_f^2 y$ are Lie derivatives. Moreover, K_P and K_D are positive definite matrices. To compute the required torques that drive the outputs to the zero, one would need to solve for τ from (13). However, since the contact force measurements are not available for the studied robot, one would need to estimate the contact forces $F = \text{col}\{F_\ell |\, \ell \in \mathcal{C}\}$. We assume a rigid contact model with the walking surface. This assumption makes the leg ends acceleration zero which can be expressed as $\ddot{p}^{\text{st}} = J(q)\, \ddot{q} + \frac{\partial}{\partial q}(J(q)\, \dot{q})\, \dot{q} = 0$, where $J(q) := \frac{\partial p^{\text{st}}}{\partial q}(q)$ is the contact Jacobian matrix. The rigid contact assumption together with (2) then yields

$$\ddot{p}^{\text{st}} = \mathrm{L}_g\mathrm{L}_f p^{\text{st}}(x)\, \tau + \mathrm{L}_w\mathrm{L}_f p^{\text{st}}(x)\, F + \mathrm{L}_f^2 p^{\text{st}}(x) = 0. \tag{14}$$

Now, we need to look for the values of (τ, F) that satisfy (13) and (14) with contact forces being in the friction cone, that is, $F_\ell \in \mathcal{FC}$ for all $\ell \in \mathcal{C}$. For this purpose, we set up the following real-time QP

$$\begin{aligned} \min_{(\tau, F, \omega)} \quad & \frac{1}{2}\|\tau\|_2^2 + \frac{\gamma}{2}\|\omega\|_2^2 \\ \text{s.t.} \quad & \mathrm{L}_g\mathrm{L}_f y\, \tau + \mathrm{L}_w\mathrm{L}_f y\, F + \mathrm{L}_f^2 y + \frac{\partial^2 y}{\partial t^2} + \omega = v_{\text{PD}}(y, \dot{y}) \\ & \mathrm{L}_g\mathrm{L}_f p^{\text{st}}\, \tau + \mathrm{L}_w\mathrm{L}_f p^{\text{st}}\, F + \mathrm{L}_f^2 p^{\text{st}} = 0 \\ & F_\ell \in \mathcal{FC}, \quad \ell \in \mathcal{C}, \quad \tau_{\min} \leq \tau \leq \tau_{\max}, \end{aligned} \tag{15}$$

in which $v_{\text{PD}}(y, \dot{y}) := -K_P\, y - K_D\, \dot{y}$ is the PD action. The equality constraints for the QP are set up based on the output dynamics (13) as well as the stance foot accelerations assumption (14). We introduce a defect variable ω in the equality constraint of QP that corresponds to the output dynamics in case the decoupling matrix $\mathrm{L}_g\mathrm{L}_f y$ is singular. To minimize the effect of the defect variable, we then add a quadratic term $\frac{\gamma}{2}\|\omega\|_2^2$ to the cost function of the QP to ensure that the 2-norm of the defect variable is as small as possible. Here, $\gamma > 0$ is a weighting factor. The other term in the cost function tries to find the minimum 2-norm (minimum power) torques that satisfy the equality and inequality constraints. Furthermore, $\tau_{\min}$ and $\tau_{\max}$ are the admissible bounds on the torques.

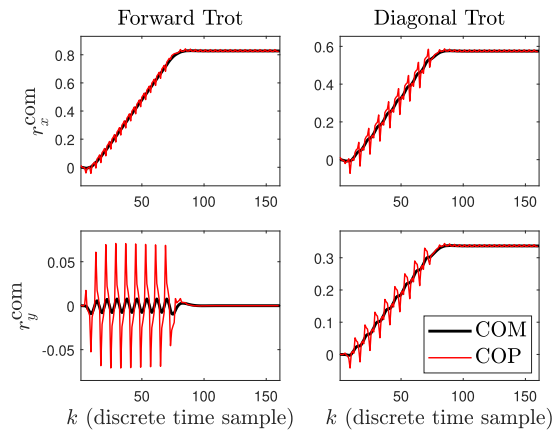

Fig. 3. Plot of the COM and COP trajectories for the forward and diagonal trot gaits of the reduced-order system. Convergence to the target points (0.82,0) and (0.58,0.34) is clear.

VI. Numerical Simulations

The objective of this section is to numerically verify the effectiveness of the theoretical results. We consider five different directions (i.e., forward, backward, sideways, diagonal, and in-place) of trot gaits with start and stop conditions whose graphs $\mathcal{G}$ consist of $M = 20$ continuous-time domains (see Fig. 2). We choose the sampling time to discretize the LIP dynamics as $T_d = 80$ (ms) with $N_d = 4$ grids per each domain. The control horizon for the event-based MPC is chosen as $N = nN_d = 8$ which considers two domains ahead. We have observed that for every T_d in [60,80] (ms) with $N_d = 4$, the proposed control scheme can stabilize the locomotion patterns. Since we prefer to have longer duration for domains of locomotion such that the lower-level controller has enough time to track the prescribed optimal motion by the MPC, we choose $T_d = 80$ (ms). The control horizon N can also be chosen to include more than two domains, but this will increase the number of decision variables and the computation time. In addition, for $N = N_d = 4$ –which only considers the current domain– the event-based MPC cannot stabilize the motion. Hence, we choose $N = 2N_d = 8$. The other parameters are taken as $P = 10^3\, I_{4\times4}$, $Q = I_4$, $R = I_{2\times2}$, and $\hat{R} = 0.01I$ that stabilize the target point for the down-sample discrete-time system (10). With the height of the COM being 0.5 (m) and the friction coefficient $\mu = 0.4$, the higher-level MPC is solved in an event-based manner, that is approximately every $N_d T_d = 0.32$ seconds. For the first, middle, and last domains, the MPC has 64, 72, and 80 decision variables, respectively, as the dimension of $\lambda_{k+i|k}$ changes per domain. Fig. 3 depicts the evolution of the COM and COP for the forward and diagonal trot gaits of the discrete-time dynamics (9) with the step lengths of (10,0) (cm) and (7,4) (cm) in $\mathbb{R}^2$, respectively. Here, we make use of ECOS QP [46] to solve the MPC in MATLAB. Convergence to the target (final) points (0.82,0) and (0.58,0.34) is clear. Target points are chosen as the geometric center of the contact points in the last domain. We remark that the proposed MPC problem of this paper has less computational load compared to [30] with $\frac{1}{3}$ of the number of decision variables that are optimized at a slower rate. Next, we study the full-order model of the robot in RaiSim [43] with rigid contact models. The lower-level QP for I-O linearization has 37 decision variables for both double- and quadruple-contact domains, which is approximately 50% of the number of decisions variables used for the higher-level QP. The lower-level QP is solved with qpSWIFT [47] in RaiSim and $\gamma = 10^7$ at every 1 (ms). The computation time of the MPC on a laptop computer with an Intel(R) Core(TM) i7-5600 U CPU 2.60 GHz (2 cores) and 8 GB of RAM is 0.2528 (ms). The low-level QP problem for the double- and quadruple-contact domains also takes 0.2334 (ms) and 0.4735 (ms), respectively. All state components of the robot, except the absolute Cartesian coordinates of the torso (i.e., p_b), are measurable by an inertial measurement unit as well as encoders. Analogous to the approach of [48], we utilize a Kalman filter to estimate p_b. Figs. 4(a) and 4(b) illustrate the evolution of the virtual constraints and torque inputs (i.e., before the gear ratio) for the full-order model of the forward and diagonal trot gaits with the maximum speed of 0.3 (m/s). To show the robustness of the control system against different contact models, the full-order model is also simulated in MATLAB/Simulink with LuGre contact models [40]. The robot still travels in a stable and robust manner towards the target. To demonstrate the robustness of the proposed control algorithm against the control frequency as well as time delays, we next assume that the control frequency is reduced from 1 kHz to 500 Hz while there is a latency of 2 (ms) in solving QPs. Fig. 4(d) illustrates the virtual constraints profile and the GRFs in one of the stance legs for this case.

Robustness Analysis: To demonstrate the robustness of the closed-loop system against payloads, we assume that there are two payloads on the robot whose masses are not known for the controller: a payload of 1.4 (kg) in the robot's EE together with a payload of 12 (kg) on the torso (40% uncertainty in the total mass). Fig. 4(c) illustrates the evolution of the virtual constraints and torques inputs versus time. It is observed that the robot is capable of rejecting the effect of uncertainties in the total mass during locomotion. To show the robustness of the proposed controller against external forces acting on the robot, we study three different scenarios in RaiSim. In the first and second simulations, we consider persistent external forces along the x- (i.e., direction walking) and y-axes (i.e., lateral direction), respectively. The forces are taken as sinusoidal disturbance inputs with the period of $0.5\,\pi = 1.57$ (s), where the magnitudes along the x- and y-axes are chosen as 30 (N) and 8 (N), respectively. In the third simulation, we investigate the balance control of the robot while being pushed from the sides. More specifically, we make use of 4 pendulums with the mass of 3 (kg) and length of 2.5 (m) that hit the robot during locomotion. The robot is capable of stable locomotion subject to the above-mentioned external forces. Figs. 5(a)–(c) depict the evolution of the virtual constraints and torque inputs versus time. To illustrate the robustness of the controller against ground height variations, we finally consider a random sequence of ground heights in the discrete set $\{\pm1, \pm2\}$ (cm) over 150 domains of blind locomotion. The time evolution of the outputs and inputs is depicted in Fig. 5(d). Animations of these simulations can be found online.[1]

[1]https://youtu.be/RJT7kJaONCc

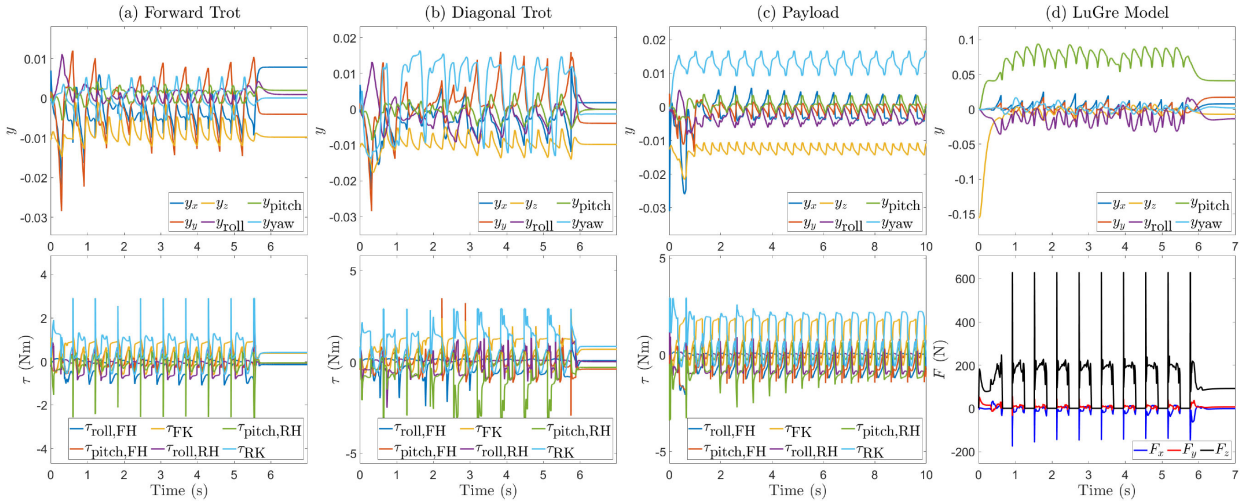

Fig. 4. Plot of the virtual constraints and torque inputs in RaiSim for (a) forward trot, (b) diagonal trot, and (c) forward trot with payloads. Here, y_x, y_y, y_z, y_{roll}, y_{pitch}, y_{yaw} denote the first six components of the virtual constraints that relate to the absolute position and orientation of the body. In addition, FH, FK, RH, and RK stand for the front hip, front knee, rear hip, and rear knee of the left-hand-side of the robot, respectively. The subscripts "roll" and "pitch" for the torque plots also denote the roll and pitch motions of the hip joints. (d) Plot of the virtual constraints and torques for trot gait subject to the LuGre contact model in MATLAB/Simulink when the control frequency is reduced to 500 Hz with a delay of 2 (ms) in solving QPs.

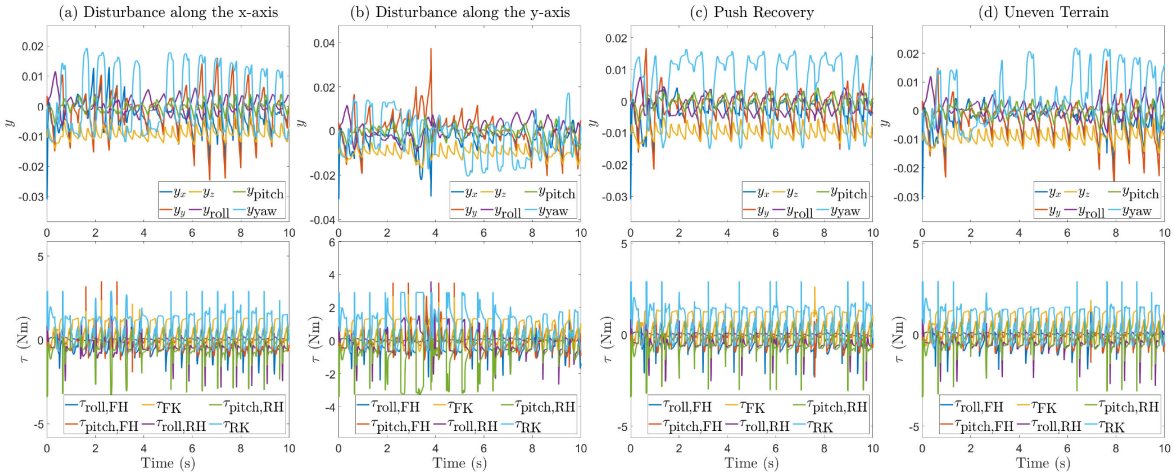

Fig. 5. Plot of the virtual constraints and torque inputs of the full-order closed-loop system in RaiSim for forward trot with (a) and (b) external disturbances, (c) external push, (d) ground height variations.

VII. Conclusion

This paper proposed a hierarchical control scheme for quadrupedal locomotion based on convex optimization, event-based MPC, and virtual constraints. At the higher level of the control scheme, the event-based MPC computes the optimal trajectory for the COM of the LIP model to steer the robot from an initial state to a final state while the net GRF is feasible. The paper addressed the asymptotic stability of the target point under the proposed MPC approach. It was formally shown that one would *not* need to employ the MPC at every time sample to stabilize the locomotion. The MPC can instead be employed in an event-based manner at the beginning of each domain to stabilize the target point. This significantly reduces the complexity for real-time implementation of MPC techniques. The lower-level controller then fills the gap between the reduced- and full-order dynamics. In particular, we formulated a QP-based I-O linearization approach to impose the full-order dynamics to follow the optimal COM trajectory of the reduced-order model while tracking the desired footholds with feasible individual GRFs. The effectiveness and robustness of the proposed control scheme were demonstrated via numerical simulations of a full-order model for a 22 DOF quadrupedal robot in the presence of payloads, external disturbances, ground height variations, and different contact models. The framework can systematically address a range of locomotion patterns such as forward, backward, lateral, diagonal, and in-place gaits. For future work, we will experimentally investigate the proposed control scheme on the Vision 60 platform. We will also study alternative gaits and terrains with inclination. Another future work will be the development of distributed controllers for the control of collaborative quadrupedal robots.

REFERENCES

[1] J. Grizzle, G. Abba, and F. Plestan, "Asymptotically stable walking for biped robots: Analysis via systems with impulse effects," *IEEE Trans. Autom. Control*, vol. 46, no. 1, pp. 51–64, Jan. 2001.

[2] A. Ames, K. Galloway, K. Sreenath, and J. Grizzle, "Rapidly exponentially stabilizing control Lyapunov functions and hybrid zero dynamics," *IEEE Trans. Autom. Control*, vol. 59, no. 4, pp. 876–891, Apr. 2014.

[3] K. Sreenath, H.-W. Park, I. Poulakakis, and J. W. Grizzle, "Compliant hybrid zero dynamics controller for achieving stable, efficient and fast bipedal walking on MABEL," *Int. J. Robot. Res.*, vol. 30, no. 9, pp. 1170–1193, Aug. 2011.

[4] S. Veer, Rakesh, and I. Poulakakis, "Input-to-state stability of periodic orbits of systems with impulse effects via Poincaré analysis," *IEEE Trans. Autom. Control*, vol. 64, no. 11, pp. 4583–4598, Nov. 2019.

[5] H. Dai and R. Tedrake, "Optimizing robust limit cycles for legged locomotion on unknown terrain," in *Proc. IEEE 51st Annu. Conf. Decis. Control*, Dec. 2012, pp. 1207–1213.

[6] C. O. Saglam and K. Byl, "Meshing hybrid zero dynamics for rough terrain walking," in *Proc. IEEE Int. Conf. Robot. Automat.*, May 2015, pp. 5718–5725.

[7] A. M. Johnson, S. A. Burden, and D. E. Koditschek, "A hybrid systems model for simple manipulation and self-manipulation systems," *Int. J. Robot. Res.*, vol. 35, no. 11, pp. 1354–1392, 2016.

[8] M. Spong and F. Bullo, "Controlled symmetries and passive walking," *IEEE Trans. Autom. Control*, vol. 50, no. 7, pp. 1025–1031, Jul. 2005.

[9] I. Manchester, U. Mettin, F. Iida, and R. Tedrake, "Stable dynamic walking over uneven terrain," *Int. J. Robot. Res.*, vol. 30, no. 3, pp. 265–279, 2011.

[10] R. Vasudevan, *Hybrid System Identification via Switched System Optimal Control for Bipedal Robotic Walking*. Berlin, Germany: Springer, 2017, pp. 635–650.

[11] K. Akbari Hamed and R. D. Gregg, "Decentralized event-based controllers for robust stabilization of hybrid periodic orbits: Application to underactuated 3D bipedal walking," *IEEE Trans. Autom. Control*, vol. 64, no. 6, pp. 2266–2281, Jun. 2019.

[12] K. Akbari Hamed, B. Buss, and J. Grizzle, "Exponentially stabilizing continuous-time controllers for periodic orbits of hybrid systems: Application to bipedal locomotion with ground height variations," *Int. J. Robot. Res.*, vol. 35, no. 8, pp. 977–999, 2016.

[13] A. D. Ames, R. D. Gregg, E. D. B. Wendel, and S. Sastry, "On the geometric reduction of controlled three-dimensional bipedal robotic walkers," in *Lagrangian and Hamiltonian Methods for Nonlinear Control 2006*. Berlin, Germany: Springer, 2007, pp. 183–196.

[14] E. Westervelt, J. Grizzle, and D. Koditschek, "Hybrid zero dynamics of planar biped walkers," *IEEE Trans. Autom. Control*, vol. 48, no. 1, pp. 42–56, Jan. 2003.

[15] A. Isidori, *Nonlinear Control Systems*. 3rd ed., Berlin, Germany: Springer, 1995.

[16] C. Chevallereau *et al.*, "RABBIT: A testbed for advanced control theory," *IEEE Control Syst. Mag.*, vol. 23, no. 5, pp. 57–79, Oct. 2003.

[17] A. Ramezani, J. Hurst, K. Akbai Hamed, and J. Grizzle, "Performance analysis and feedback control of ATRIAS, a three-dimensional bipedal robot," *J. Dyn. Syst., Meas. Control Dec., ASME*, vol. 136, no. 2, pp. 021012-1–021012-12, Dec. 2013.

[18] A. Hereid, C. M. Hubicki, E. A. Cousineau, and A. D. Ames, "Dynamic humanoid locomotion: A scalable formulation for HZD gait optimization," *IEEE Trans. Robot.*, vol. 34, no. 2, pp. 370–387, Apr. 2018.

[19] A. E. Martin, D. C. Post, and J. P. Schmiedeler, "The effects of foot geometric properties on the gait of planar bipeds walking under HZD-based control," *Int. J. Robot. Res.*, vol. 33, no. 12, pp. 1530–1543, 2014.

[20] R. Gregg and J. Sensinger, "Towards biomimetic virtual constraint control of a powered prosthetic leg," *IEEE Trans. Control Syst. Technol.*, vol. 22, no. 1, pp. 246–254, Jan. 2014.

[21] H. Zhao, J. Horn, J. Reher, V. Paredes, and A. D. Ames, "Multicontact locomotion on transfemoral prostheses via hybrid system models and optimization-based control," *IEEE Trans. Automat. Sci. Eng.*, vol. 13, no. 2, pp. 502–513, Apr. 2016.

[22] A. Agrawal *et al.*, "First steps towards translating hzd control of bipedal robots to decentralized control of exoskeletons," *IEEE Access*, vol. 5, pp. 9919–9934, 2017.

[23] K. Akbari Hamed, W. Ma, and A. D. Ames, "Dynamically stable 3D quadrupedal walking with multi-domain hybrid system models and virtual constraint controllers," in *Proc. Amer. Control Conf.*, Jul. 2019, pp. 4588–4595.

[24] R. J. Griffin, G. Wiedebach, S. Bertrand, A. Leonessa, and J. Pratt, "Walking stabilization using step timing and location adjustment on the humanoid robot, Atlas," in *Proc. IEEE/RSJ Int. Conf. Intell. Robots Syst.*, Sep. 2017, pp. 667–673.

[25] J. Englsberger, C. Ott, M. A. Roa, A. Albu-Schffer, and G. Hirzinger, "Bipedal walking control based on capture point dynamics," in *Proc. IEEE/RSJ Int. Conf. Intell. Robots Syst.*, Sep. 2011, pp. 4420–4427.

[26] S. Kajita *et al.*, "Biped walking pattern generation by using preview control of zero-moment point," in *Proc. IEEE Int. Conf. Robot. Automat.*, Sep. 2003, vol. 2, pp. 1620–1626.

[27] J. Pratt, J. Carff, S. Drakunov, and A. Goswami, "Capture point: A step toward humanoid push recovery," in *Proc. 6th IEEE-RAS Int. Conf. Humanoid Robots*, Dec. 2006, pp. 200–207.

[28] M. Vukobratović, B. Borovac, and D. Surla, *Dynamics of Biped Locomotion*. Berlin, Germany: Springer, 1990.

[29] J. Di Carlo, P. M. Wensing, B. Katz, G. Bledt, and S. Kim, "Dynamic locomotion in the MIT Cheetah 3 through convex model-predictive control," in *Proc. IEEE/RSJ Int. Conf. Intell. Robots Syst.*, Oct. 2018, pp. 1–9.

[30] Y. Ding, A. Pandala, and H. Park, "Real-time model predictive control for versatile dynamic motions in quadrupedal robots," in *Proc. Int. Conf. Robot. Automat.*, May 2019, pp. 8484–8490.

[31] O. Villarreal, V. Barasuol, P. Wensing, and C. Semini, "MPC-based controller with terrain insight for dynamic legged locomotion," in *Proc. Int. Conf. Robot. Automat.*, 2020, *arXiv:1909.13842*.

[32] M. Neunert *et al.*, "Whole-body nonlinear model predictive control through contacts for quadrupeds," *IEEE Robot. Automat. Lett.*, vol. 3, no. 3, pp. 1458–1465, Jul. 2018.

[33] G. Bledt, P. M. Wensing, and S. Kim, "Policy-regularized model predictive control to stabilize diverse quadrupedal gaits for the mit cheetah," in *Proc. IEEE/RSJ Int. Conf. Intell. Robots Syst.*, Sep. 2017, pp. 4102–4109.

[34] S. Fahmi, C. Mastalli, M. Focchi, and C. Semini, "Passive whole-body control for quadruped robots: Experimental validation over challenging terrain," *IEEE Robot. Automat. Lett.*, vol. 4, no. 3, pp. 2553–2560, Jul. 2019.

[35] S. Kuindersma, F. Permenter, and R. Tedrake, "An efficiently solvable quadratic program for stabilizing dynamic locomotion," in *Proc. IEEE Int. Conf. Robot. Automat.*, May 2014, pp. 2589–2594.

[36] D. Lehmann, E. Henriksson, and K. H. Johansson, "Event-triggered model predictive control of discrete-time linear systems subject to disturbances," in *Proc. Eur. Control Conf.*, 2013, pp. 1156–1161.

[37] A. W. Winkler, F. Farshidian, D. Pardo, M. Neunert, and J. Buchli, "Fast trajectory optimization for legged robots using vertex-based ZMP constraints," *IEEE Robot. Automat. Lett.*, vol. 2, no. 4, pp. 2201–2208, Oct. 2017.

[38] D. Kim, J. D. Carlo, B. Katz, G. Bledt, and S. Kim, "Highly dynamic quadruped locomotion via whole-body impulse control and model predictive control," 2019, *arXiv:1909.06586*.

[39] E. Westervelt, J. Grizzle, C. Chevallereau, J. Choi, and B. Morris, *Feedback Control of Dynamic Bipedal Robot Locomotion*. New York, NY, USA: Taylor & Francis, 2007.

[40] C. De Wit, H. Olsson, K. Astrom, and P. Lischinsky, "A new model for control of systems with friction," *IEEE Trans. Autom. Control*, vol. 40, no. 3, pp. 419–425, Mar. 1995.

[41] D. E. Stewart and J. C. Trinkle, "An implicit time-stepping scheme for rigid body dynamics with inelastic collisions and coulomb friction," *Int. J. Numerical Methods Eng.*, vol. 39, no. 15, pp. 2673–2691, 1996.

[42] E. Todorov, T. Erez, and Y. Tassa, "MuJoCo: A physics engine for model-based control," in *Proc. IEEE/RSJ Int. Conf. Intell. Robots Syst.*, Oct. 2012, pp. 5026–5033.

[43] J. Hwangbo, J. Lee, and M. Hutter, "Per-contact iteration method for solving contact dynamics," *IEEE Robot. Automat. Lett.*, vol. 3, no. 2, pp. 895–902, Apr. 2018.

[44] Y. Wang and S. Boyd, "Fast model predictive control using online optimization," *IEEE Trans. Control Syst. Technol.*, vol. 18, no. 2, pp. 267–278, Mar. 2010.

[45] L. Coroianu, "Best Lipschitz constants of solutions of quadratic programs," *J. Optim. Theory Appl.*, vol. 170, no. 3, pp. 853–875, Sep. 2016.

[46] A. Domahidi, E. Chu, and S. Boyd, "ECOS: An SOCP solver for embedded systems," in *Proc. Eur. Control Conf.*, Jul. 2013, pp. 3071–3076.

[47] A. G. Pandala, Y. Ding, and H. Park, "qpSWIFT: A real-time sparse quadratic program solver for robotic applications," *IEEE Robot. Automat. Lett.*, vol. 4, no. 4, pp. 3355–3362, Oct. 2019.

[48] G. Bledt, M. J. Powell, B. Katz, J. Di Carlo, P. M. Wensing, and S. Kim, "MIT Cheetah 3: Design and control of a robust, dynamic quadruped robot," in *Proc. IEEE/RSJ Int. Conf. Intell. Robots Syst.*, Oct. 2018, pp. 2245–2252.